5

Superiority of activated graphite/CuO composite electrode over Platinum based electrodes as cathode in algae assisted microbial fuel cell

Oxygen reduction reaction (ORR) at the cathode surface is essential for continuous power production in a MFC. However, oxygen reduction at the cathode surface is slow and has high overpotential. This in turn affects the MFC performance and results in low power outputs [Bhowmick et al., 2019].

Chemical fuel cells often employ platinum (Pt) catalysts on electrode surface. It enhances the ORR and boosts power output. However, the use of Pt is not feasible in MFCs because of the use of phosphate, nitrate, and chloride salts as growth medium components for microbes. These ions poison Pt, lowering its catalytic efficiency [Yi et al., 2019]. In addition, Pt is toxic and too expensive to be used for a bioenergy or bioremediation process.

In this context, researchers have made several attempts to develop low-cost, high efficiency catalyst for enhancing ORR. Recently, a study reported cathode catalyst using ZnO-NiO modified with rGO (reduced graphene oxide) and employed it in algae assisted MFC. The electrode supported better electrochemical activity [Liu et al., 2019]. One study reported a bimetallic N-doped Cu/Co composite with a carbon framework for ORR in MFC. The catalyst showed enhanced electrochemical activity and power density of 1008 mW/m^2, which was 1.31 times higher than Pt/C electrode [H. Wang et al., 2020].

Similarly, the use of transition metals, their alloys, and oxides based nanoparticles (NPs) have been increased recently as these have high charge density [Askari and Salarizadeh, 2019; Askari et al., 2019; Cheng et al., 2017; Das et al., 2020a; Lee et al., 2012; Salarizadeh et al., 2019; Salarizadeh et al., 2020]. For example, Cu-Sn NPs, Ag_3Pt, and Cu-Zn NPs improve ORR as indicated in several studies [Das et al., 2020b; Noori et al., 2018a; Noori et al., 2018b]. The Cu based NPs have been extensively employed as cathodic catalysts in fuel cells. For example, N-type Cu_2O doped activated carbon has been reported to enhance cathodic ORR with a 1390 mW/m^2 as power density [Zhang et al., 2015]. Similarly, Cu_2O/rGO composite cathode exhibited improved electrochemical activity, higher columbic efficiency and promoted more microbial growth at the electrode surface than that of commercially available Pt/C [Xin et al., 2020]. Although there are several reports of utilizing Cu_2O as a catalyst in chemical fuel cell but there is barely any report on their suitability for MFCs. In addition, the metal oxides and their alloys may be toxic, limiting their applications in MFCs, particularly based on biocathodes. Therefore, this study was undertaken to address the following objectives: -

1. To assess the potential and suitability of activated graphite/CuO, Fe_3O_4, MnO_2 NPs composite electrode as the cathode in algae assisted MFCs.

2. To compare their performance with Pt/C based electrode in terms of power output and algal growth.

5.1 MFC inoculation and operation

The membrane filtration units (make Tarson, volume 250 ml) were used as MFCs (Figure 5.1). The lower chamber served as anode and the upper one as the cathodic chamber. The chambers were separated by an ultra-filtration membrane (diameter 47 mm). Graphite felt (4 cm × 4 cm × 0.56 cm) was used as an anode. The cathode was made of a graphite powder mixed with CuO nanoparticles (Diameter- 1.3 cm, height- 0.8 cm). To prepare the cathode, the graphite powder was treated with nitric acid as described previously [Erable et al., 2009]. Three types of MFCs, namely G-MFC (graphite only), G-N-MFC (Graphite treated with nitric acid), and G-N-CuO-MFC (Nitric acid treated graphite and CuO NPs composite). The fourth type consisted of Pt coated carbon cloth (0.5 mg/cm^2, 4 cm × 4cm) as a cathode material (Pt-MFC). Anolyte was used as described previously [Vijay et al., 2016] and BG-11 media was utilized to grow algae in the cathodic chamber. Cow-manure was used as a source of electrogens and inoculated in the anodic chamber, while the cathodic compartment was inoculated with microalgae *Chlorella vulgaris*. MFCs were operated in fed-batch mode and in every new batch cycle, all the MFC reactors were supplemented with fresh media and fruit pulp (2g/l) as a substrate for anodic exo-electrogenic bacteria.

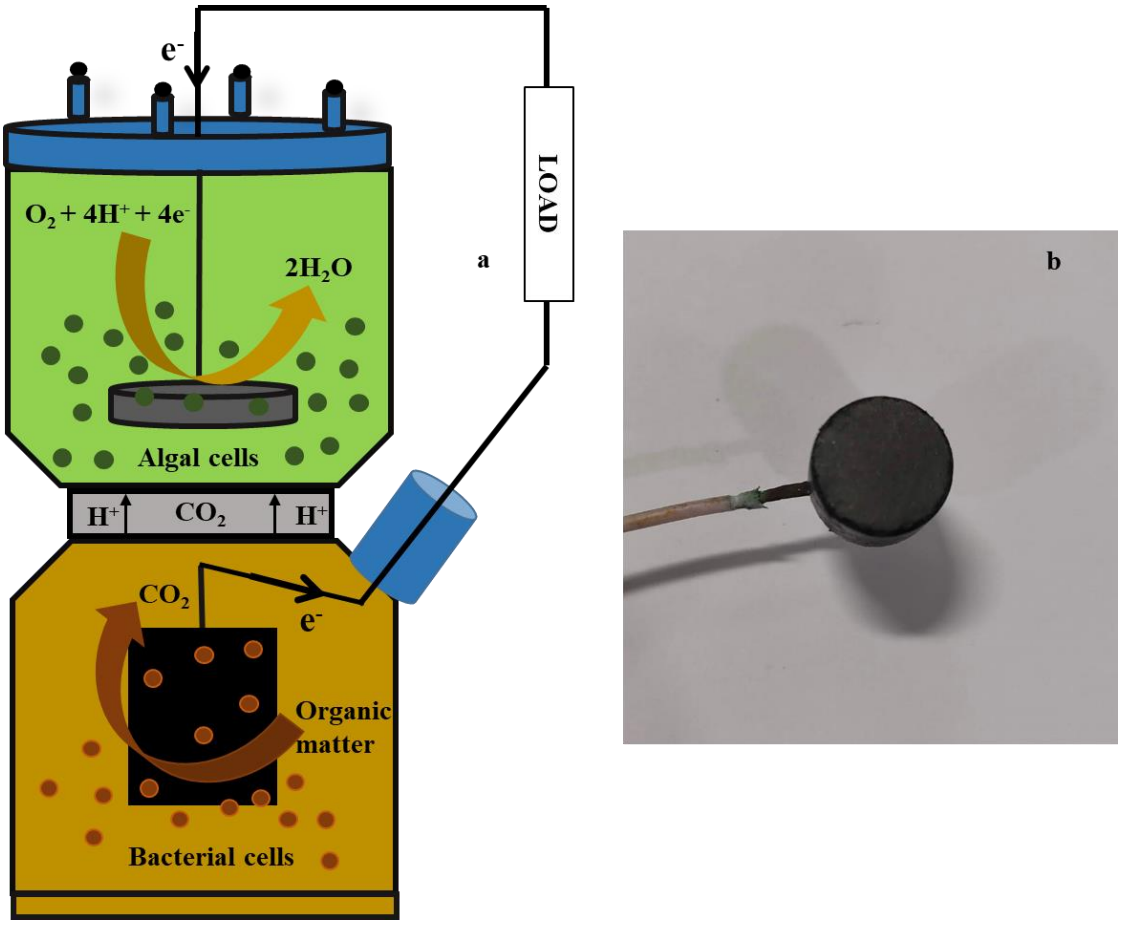

Figure 5.1: a) Schematic of the top-bottom configuration of MFC reactor employed in the study, and b) fabricated composite electrode.

5.2 RESULTS AND DISCUSSIONS

5.2.1 Physical characterization

Figure 5.2 is showing the XRD pattern observed for all the three nano-particles, pure graphite and graphite powder modified with CuO NPs. The XRD pattern of β-MnO_2 NPs displayed distinguished peaks at 2θ = 28.7°, 37.5°, 42°, 60° and 70° which are associated to 110, 101, 200, 220 and 221 planes respectively (Figure 5.2 a). The XRD pattern observed for MnO_2 NPs is in agreement with the previously reported study [Zhou et al., 2018]. Similarly, the XRD spectrum of Fe_3O_4 NPs showed a distinctive peak linked to 311 hkl plane (Figure 5.2b), which is also aligned with the literature [Sivakumar et al., 2018]. Furthermore, the CuO NPs exhibited the prominent XRD peaks at 2θ = 32.46°, 35.44°, 38.7°, 48.7° and 61.58°. These peaks are corresponding to (110), (-110), (111), (-202) and (-113) planes of the monoclinic structure of CuO (Figure 5.2c). The 2θ value and their corresponding hkl values are in accordance with the previously reported studies [Christy et al., 2013; Wang et al., 2019]. For graphite sample, the characteristic XRD peak was obtained at 2θ = 26.46° which belongs to (002) plane of graphite (Figure 5.2d). Moreover, for the graphite/CuO composite four major peaks were recorded at 2θ = 26.5°, 35.44°, 38.64° and 48.7° (Figure 5.2e). The XRD peak at 2θ = 26.5° shows the presence of graphite (002), which depicts the stacks formed due to conjugation of double bonds [Zhang et al., 2020]. In addition to this, the rest of XRD peaks observed in the graphite/CuO composite are similar to that of obtained in the X-ray diffractogram of CuO NPs, which confirms that CuO NPs are successfully incorporated in the graphite.

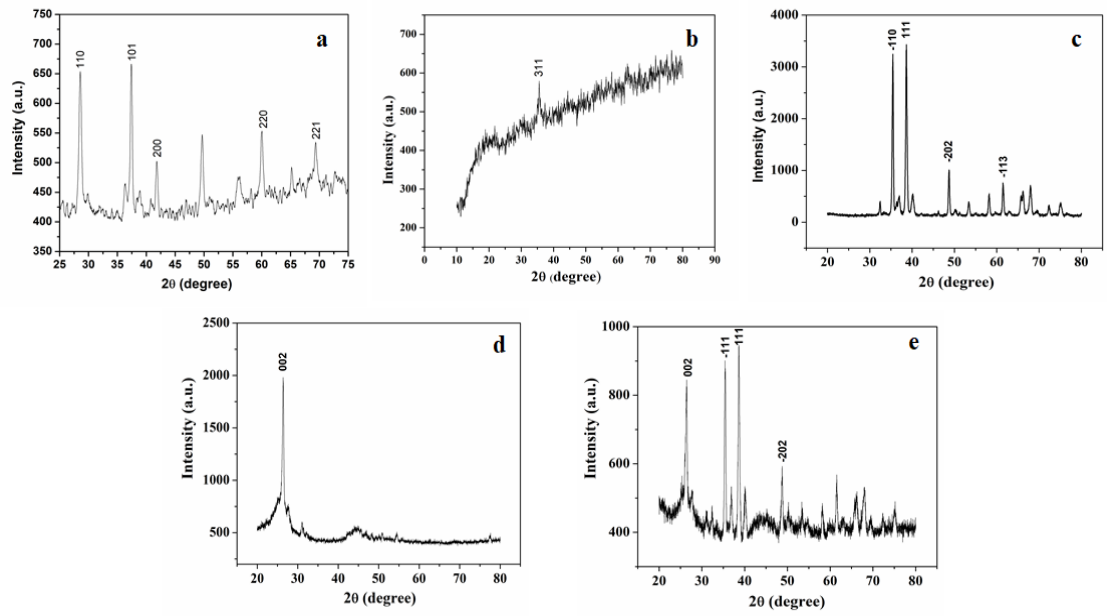

Figure 5.2: XRD graphs obtained for a) MnO2 NPs, b) Fe3O4 NPs, c) CuO NPs, d) pristine graphite, and e) composite graphite/CuO.

SEM analysis was carried out to understand the surface morphology of synthesized NPs and fabricated electrodes. SEM images obtained for CuO NPs disclosed its rod like structure with an average size of 20-25 nm width and 200-250 nm length (Figure 5.3a). Similarly, the β-MnO_2 NPs exhibited a nano-rod structure, with a diameter of 200-250 nm and length 600-700 nm (Figure 5.3b). The Fe_3O_4 NPs displayed uniform sized globular particles (Figure 5.3c). Figure 5.3d reveals that the graphite possesses an uneven surface morphology. Several flakes of graphite and granules of small graphitic particles can be seen scattered irregularly over the

surface of the electrode. In addition, varying sizes of interplanar microcrystalline are visible which led to the conclusion that graphite is a multi-layered structure. On the other hand, the graphite/CuO composite exhibited the cluster of flakes aggregated together. The aggregation of flakes is possibly the result of nitric acid treatment (Figure 5.3e). The EDX elemental mapping obtained from SEM revealed the presence of carbon, oxygen, and copper in the fabricated electrode (Figure 5.3f, 5.3h, 5.3i, 5.3j, 5.3k) conforming the successful fabrication of composite electrode.

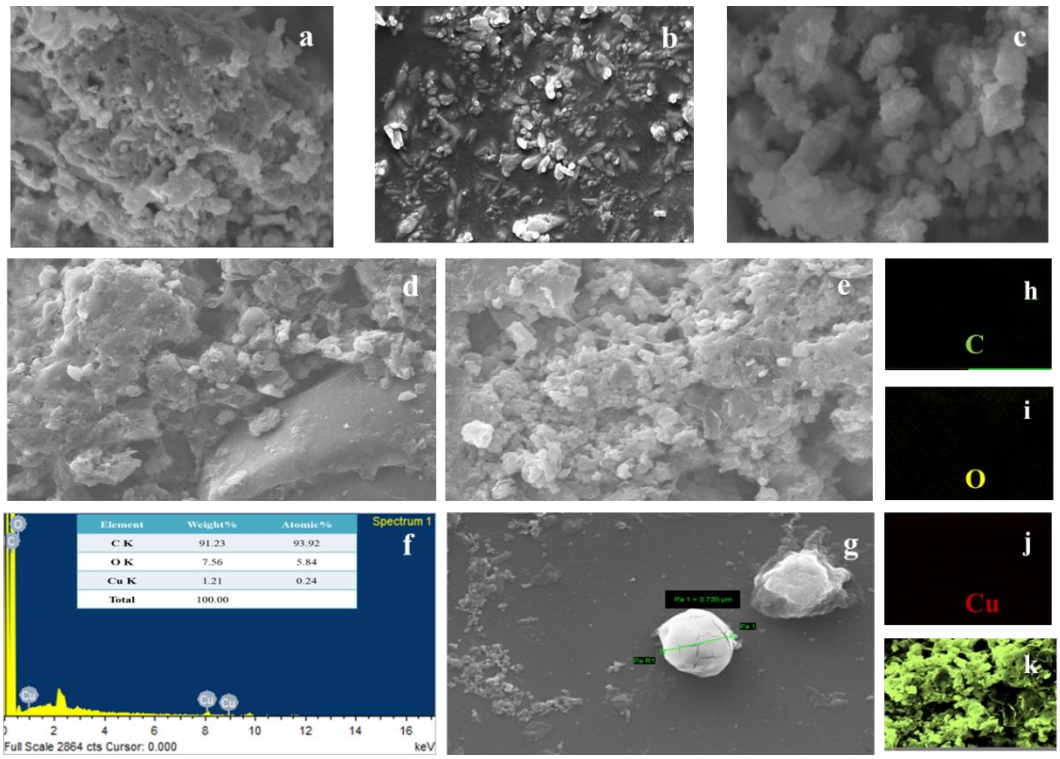

Figure 5.3: SEM images of a) CuO NPs, b) MnO_2 NPs, c) Fe_3O_4 NPs, d) pure graphite electrode, e) graphite/CuO composite electrode, f) EDX spectra of graphite/CuO composite electrode, g) algal cells on composite electrode, and h, i, j, k) EDX elemental mapping.

5.2.2 Voltage and Polarization behaviour

The operating voltage across the 1000 ohm resistor increased with the progression of each batch cycle. Table 5.1 summarizes the key results obtained for different Nano-particles. The 20% CuO composite electrode outperformed other electrodes in terms of voltage, power density, algal growth, and electrochemical activity. The voltage values were observed as 380 ± 7, 270 ± 12, 220 ± 5 and 205 ± 20 mV in G-N-CuO MFC, G-N-MFC, G-MFC, and Pt-MFC respectively. The oscillation in the voltage profile was due to oscillatory dissolved oxygen concentrations resulting from light/dark period. The G-N-CuO MFC gave the highest OCV and operating voltage (Table 5.1). The power and current density were in the order of 6 W/m^3 and 25 A/m^3 in G-N-CuO MFC (Figure 5.4). The G-N-MFC, G-MFC and Pt-MFC gave 3.6 W/m^3, 1.75 W/m^3, and 1.35 W/m^3 of power density. This was 1.6, 3.4 and 4.4 times lower than G-N-CuO MFC. The Pt-MFC also did not support algae growth, which in turn affected DO concentration and voltage.

Recently, a Cu_2O nano-particles composite with reduced grapheme oxide was employed in a single chamber MFC as a cathode catalyst and it exhibited 223 mV as operating voltage [Xin

et al., 2020]. Similarly, a Cu/Co/N co-doped carbon hollow sphere based cathode catalyst showed output voltage 620 mV as output voltage and 1.01 W/m^2 as power density [H. Wang et al.,, 2020b]. Furthermore, a power density of 1.2 W/m^2 was obtained using Co/N@ C as cathode catalyst. In the present study, only activated graphite was utilized as a carbon source which is cheaper than other carbon based materials such as graphene, graphene oxide, reduced graphene oxide, etc.

Table 5.1: Table showing comparative results obtained for different NPs used in varying concentrations in MFC reactors.

Cathode material	Open circuit voltage (mV)	Voltage at 1000 Ω (mV)	Power Density (W/m^3)	COD Degradation rate (kg/m^3/d)	Algae growth rate μ (d^{-1})	Cathode potential (mV)	Anode potential (mV)
10% CuO	269±34	120.5±4	0.41±0.01	0.185±0.01	0.229±0.03	118±5	-151±2.6
20% CuO	**840±10**	**380 ± 7**	**6 ±0.2**	**0.185± 0.005**	**0.246±0.014**	**377±4**	**-465±3**
30% CuO	506±36	260±9	3.7±0.1	0.166 ±0.017	0.198±0.02	154±6.2	-352±4
10% MnO_2	611±31	251±5	2.1±0.05	0.169 ±0.042	0.187±0.014	252±8	-363±3.4
20% MnO_2	459±53	202±6	1.1±0.05	0.129± 0.06	0.194±0.018	185±4.2	-275±7
30% MnO_2	510±60	230±10	2.9±0.13	0.174±0.007	0.114±0.016	143±2	-367±5
10% Fe_3O_4	415±58	184±4	2.1±0.1	0.210±0.007	0.125±0.014	261±7	-156±2.9
20% Fe_3O_4	348±50	213±2	3.2±0.03	0.196±0.004	0.234±0.016	218±3.6	-130±3.7
30% Fe_3O_4	381±21	194±7	1.3±0.05	0.185±0.009	0.220±0.012	189±5.2	-192±4.4
Mix	611±25	265±5	3.4±0.35	0.179±0.019	0.239±0.016	252±6	-359±2
Pt/C	620±38	205±8	1.35±0.1	0.182±0.020	0.145	382±2	238±6

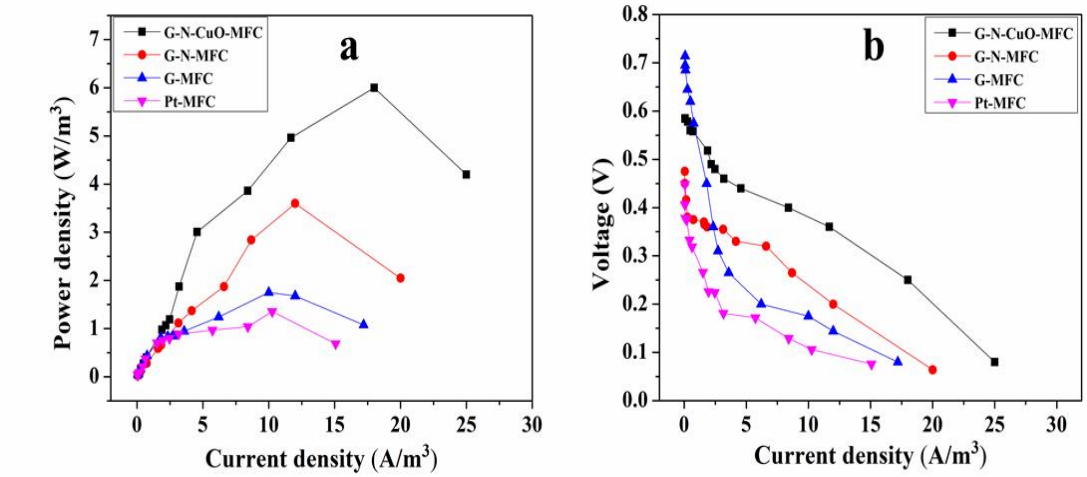

Figure 5.4: Polarization curves obtained for different MFC reactors.

5.2.3 Algal growth

The algae assisted MFC relies on algae growth and oxygen liberation through the action of photosynthesis. Higher algae growth rates are useful for power output and biomass production. The specific growth rate observed for *C. vulgaris* was 0.239 d^{-1}, 0.259 d^{-1}, 0.256 d^{-1}, and **0.145 d^{-1}** for G-MFC. G-N-MFC, G-N-Cu0 MFC, and Pt-MFC respectively. The G-N-MFC and G-N-CuO-MFC supported almost equal cell density and reached a cell number of 1130 ± 44 × 10^4 cells/ml

and 1050 ± 37 × 10^4 cells/ml respectively. G-MFC attained a cell density of 978 ± 48 × 10^4 cells/ml. The, Pt-C based MFC reactor could attain only 700 ± 35 × 10^4 cells/ml on the 10^{th} day (Figure 5.5). The algae cell also showed visible discoloration turning from green to blue and then brown over the incubation period. Similar observations have been made earlier. It was observed that Pt decreased the chlorophyll content which led to a reduction in cell density of a freshwater microalgae *Pseudokirchneriella subcapitata* [Książyk et al., 2015]. Sorensen et al., (2016), investigated the toxic effect of Pt on *Chlamydomonas reinhardtii* and *P. subcapitata* and concluded that Pt caused oxidative stress as well as growth rate inhibition in both the algal species. The possible mechanism for this involves attachment of Pt to the algal cell surface leading to shading effect and/or intervention in membrane associated processes such as nutrient uptake etc. However, the sensitivity towards Pt toxicity varies from species to species [Sørensen et al., 2016]. Similarly, Intrchom et al., (2018) studied the effect of carbon nano tube (CNT)-Pt hybrid complex on *C. reinhardtii* and observed that CNT-Pt inhibited the algal growth by 73% and 79% at the concentration of 0.5 mg/l and 5 mg/l, respectively, compared to that of control [Intrchom et al., 2018]. Hence, it can be concluded that Pt coated electrodes are not suitable for enhancing ORR in algae based MFCs.

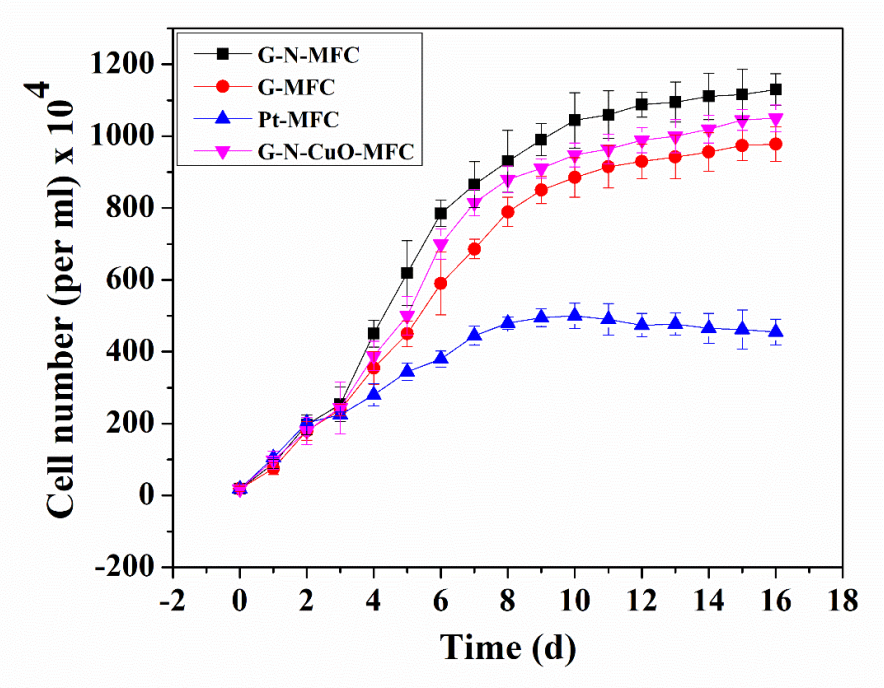

Figure 5.5: Algal growth kinetics observed for different MFC reactors.

5.2.4 Electrochemical analysis

Cyclic voltammetry (CV) was done in order to evaluate the electrocatalytic activity of the fabricated electrodes. CV is a powerful tool which helps to understand the exact mechanism through which the redox reaction takes place at the electrode surface. As shown in figure 5.6a, Pt coated carbon cloth showed a sharp peak at 0.10 V with a cathodic current density of 0.13 mA/cm^2. The distinguishable reduction peaks were not seen in G-MFC and G-N-MFC (Figure 5.6b). However, the G-N-CuO-MFC showed two prominent reduction peaks at 0.13 V and 0.10 V with a reduction current value of 0.416 mA/cm^2 and 0.445 mA/cm^2 respectively. The G-N-CuO-MFC also displayed a broad oxidation peak at 0.04 V. The reduction current realized in

graphite/CuO composite electrode is higher than that of Pt-C electrode. Copper is known to effectively mediate oxygen reduction at cathode.

In principle, the molecular oxygen reduction either follows an efficient 4 electron reduction path which leads to the formation of OH^- ions or a 2 electron reduction with an intermediate HO_2^- ion.

The possible mechanism for the reaction occurring at the composite/Cuo surface may be as follows:-

$$2CuO + OH^- + 2e^- \longrightarrow Cu_2O + 2OH^- \quad (5.1)$$ [Zhang et al., 2015].

The graphite/CuO composite electrode showed a higher reduction area as well as the higher cathodic current which prove its superiority over Pt based electrodes. Inhibition of algae by Pt leads to low DO levels, leading to low cathodic currents and peak areas. The first derivative from CV also suggested graphite/CuO composite better than Pt/C for ORR in algae assisted MFCs.

Although there are numerous reports on cheaper alternatives for promoting cathodic ORR but most of them employed air-cathodes in their studies. There is barely any report on cathode fabrication for catalyzing ORR in biocathodes. However, recently Liu et al., (2019) fabricated a carbon felt cathode with ZnO-NiO@rGO in an algae assisted MFC. Both ZnO & NiO are known to be good semiconductor therefore, enable the adsorption of oxygen which leads to enhance charge transfer ability & electrochemical activity [Liu et al., 2019]. Similarly, the CuO NPs is a p-type semiconductor material having a narrow bandwidth of 1.2 eV [Priya and Berchmans, 2012], which resulted in higher cathodic catalytic activity in this study.

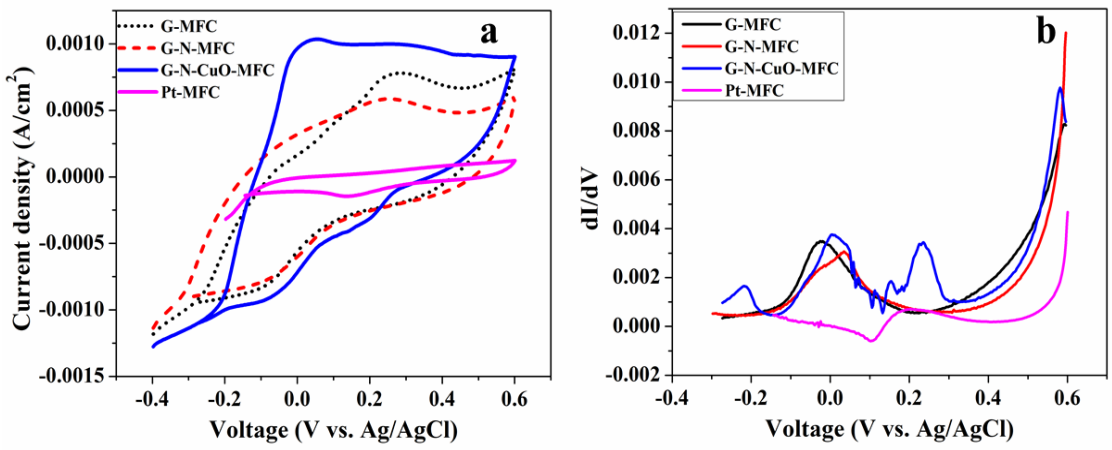

Figure 5.6: Cyclic voltammograms a) CV curves normalized by cathodic surface area, and b) first derivative of reverse scan of CV curves.

5.2.5 Fatty acid profile of cathodic algae

In order to check the lipid profile of algae biomass grown in the cathodic chamber, the lipids were extracted from algal biomass following the protocol described previously [Kanaga et al., 2016]. The extracted lipids were converted to FAME (fatty acid methyl ester) and subjected to GC-MS analysis. The total saturated fatty acids (SFA) were observed as 24.16 ± 1.75%, while the total unsaturated fatty acids (UFA) were found to be 53.29 ± 3.14%. The SFA value (24.16 ± 1.75%) was significantly higher than that of other vegetable oils such as soyabean oil (15%), rapeseed oil (6.6%), jatropha oil (21.52%) and sunflower oil (4.5%) [Vyas and Chhabra, 2017].

The chain length and degree of saturation in fatty acids are crucial parameters determining oxidative stability, cetane number, and kinetic viscosity of the biodiesel [Sitepu et al., 2014]. The palmitic acid ($C_{16:0}$) was observed as 18.79 ± 0.82% which is higher than that of soyabean oil (11%) and jatropha oil (14.66%). Similarly, the Palmitoleic acid was 1.68 ± 0.08%, which is also greater than that of yeast based biofuel (0.43%) [Vyas and Chhabra, 2017]. The oleic acid ($C_{18:1}$)) 12.30 ± 0.46%), and stearic acid ($C_{18:0}$) (5.37 ± 0.935%) concentrations were also comparable to that of vegetable oils (4-6%). The linoleic acid ($C_{18:2}$) 14.61 ± 0.720%, linolenic acid ($C_{18:3}$) and arachidic acid ($C_{20:0}$) were found to be 14.61 ± 0.720%, 24.70 ± 1.410% and 5.94 ± 2.280%, respectively. In summary, the fatty acid profiles were suitable for biodiesel production.

Table 5.2: Summary of the results obtained from different MFC reactors.

Parameters	G-MFC	G-N-MFC	G-N-CuO-MFC	Pt-MFC
OCV (mV)	650 ± 15	785 ± 25	840 ± 10	620 ± 38
Operating voltage (mV)	220 ± 5	270 ± 12	380 ± 7	205 ± 20
Power density (W/m^3)	1.75	3.6	6	1.35
Current density (A/m^3)	17.2	20	25	15
Power density (W/m^2)	0.136	0.281	0.507	0.043
Current density (A/m^2)	1.34	2.50	3.12	0.53
Specific algal growth rate (d^{-1})	0.239	0.259	0.256	0.145

5.3 Conclusions

The results of the study suggested that graphite/CuO composite is superior over Pt/C when used in algae based MFCs cultivating *Chlorella vulgaris*. Further studies will be needed to adequately blend graphite and metal oxide nanoparticles and test its efficacy in scaled up systems. This also involves complete electrochemical characterization of graphite electrodes embedded metal oxide nanoparticles.

...